C. T. Hayes[1], Alan M. Shiller[1] and Scott P. Milroy[1]

[1]School of Ocean Science and Engineering, University of Southern Mississippi, Stennis Space Center, MS, USA

Corresponding author: Christopher Hayes (`christopher.t.hayes@usm.edu`)

Key Points:

- An upper bound on the contribution of North African dust toward dissolved thorium supply in the northern Gulf of Mexico may be around 30%

- Thorium and other tracers suggest significant additional sources from benthic sediment flux and/or submarine groundwater discharge

- Thorium-based lithogenic supply of iron suggests dissolved iron residence time in the northern Gulf of Mexico is less than 6 months

Plain Language Summary

The ocean's nutrients generally come from land. The specific route a nutrient takes depends on the nutrient. For the nutrient iron, the rain of airborne dust blown from deserts is thought to be a significant source, especially in the remote ocean. This is because iron is very insoluble and cannot travel far in the water. The Gulf of Mexico is a semi-enclosed sea with significant contact with ocean sediments. It is uncertain how this margin source might compare to airborne dust in the Gulf of Mexico. In this study we used another element, thorium, to trace these two sources and found that dust is likely a significant but not dominant source.

Abstract

North African dust is known to be deposited in the Gulf of Mexico, but its deposition rate and associated supply of lithogenic dissolved metals, such as the abiotic metal thorium or the micronutrient metal iron, have not been well-quantified. ^{232}Th is an isotope with similar sources as iron and its input can be quantified using radiogenic ^{230}Th. By comparing dissolved ^{232}Th fluxes at three sites in the northern Gulf of Mexico with upwind sites in the North Atlantic, we place an upper bound on North African dust contributions to ^{232}Th and Fe in the Gulf of Mexico, which is about 30%. Precision on this bound is hindered by uncertainty in the relative rates of dust deposition in the North Atlantic and the northern Gulf of Mexico. Submarine groundwater discharge and benthic sedimentary releases are likely as important if not more important than dust in the budget of lithogenic metals in the Gulf of Mexico. Our estimated Fe input in the northern Gulf of Mexico implies an Fe residence time of less than 6 months, similar to that in the North Atlantic despite significantly higher supply rates in the Gulf of Mexico.

1 Introduction

The transfer of material from land to sea is one of the primary drivers of the chemical composition of the ocean. There are five main pathways through which this transfer occurs: river discharge, atmospheric deposition, release from sediments, submarine groundwater discharge, and hydrothermal activity (Jeandel, 2016). Any given chemical element in the ocean was delivered from some mixture of these sources and any constraint on the absolute or relative magnitude of each source improves our ability to predict its behavior. The Gulf of Mexico is in some regards a model ocean to study with respect to chemical sources, with supplies from all the major pathways. The Gulf of Mexico receives material input from: one of the world's largest rivers in terms of sediment discharge, the Mississippi River (Milliman & Meade, 1983); atmospheric deposition of North African dust (Prospero, 1999; Prospero et al., 2010) and North American aerosol (Bozlaker et al., 2019; Kok et al., 2021a); a sediment-laden continental shelf that occupies one third of its seafloor; and submarine groundwater discharge in both the northern (McCoy & Corbett, 2009) and southern (Gonneea et al., 2014) margins. Hydrothermal activity is not known within the Gulf of Mexico, although it potentially receives material of hydrothermal origin from upstream vent sites on the Mid-Cayman Rise (Kinsey & German, 2013; McDermott et al., 2018) in the Caribbean Sea.

We are motivated to constrain lithogenic sources in the Gulf of Mexico, as sources of trace metals in particular, because of their impact on marine ecosystems. Biological productivity in much of the Gulf is likely limited by supply of the major nutrient nitrogen (Yingling et al., 2021; Zhao & Quigg, 2014). However, there is some evidence that availability of the micronutrient, iron, which is heavily impacted by lithogenic sources (Tagliabue et al., 2017), may alter phytoplankton communities on the West Florida Shelf (see map in Fig. 1) through the high-iron requirement of nitrogen-fixing cyanobateria (Lenes et al., 2001; Walsh et al., 2006). It has been shown that dissolved Fe concentrations on the West Florida Shelf can become elevated during a season of higher North African dust deposition (Mellett & Buck, 2020). However, Gulf of Mexico coastal waters in general are known to be enriched in trace metals compared to its interior waters (Boyle et al., 1984; Joung & Shiller, 2016; Lenes et al., 2001; Mellett & Buck, 2020; Tang et al., 2002; Wen et al., 2011). Thus it can be difficult to ascribe sources from trace metal data alone.
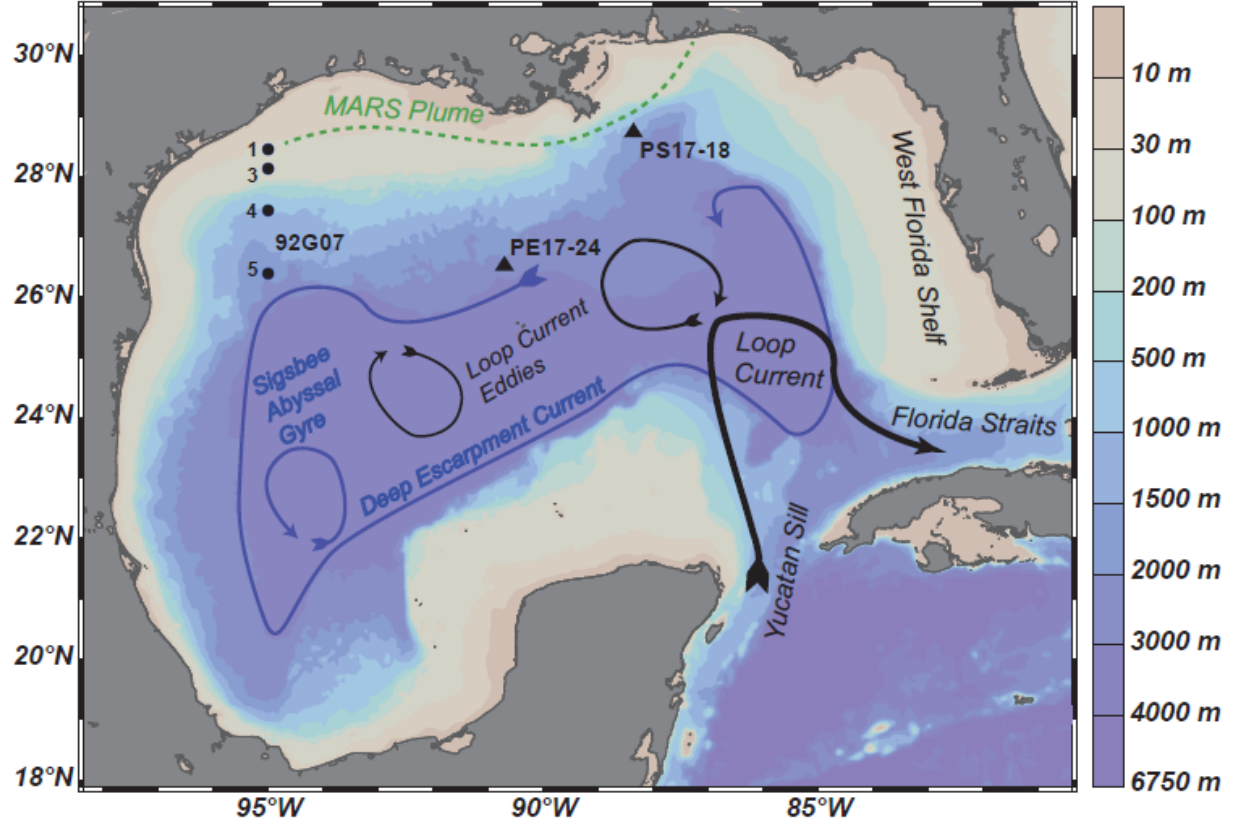
Figure 1. Gulf of Mexico study sites presented here for dissolved ^{232}Th and ^{230}Th (black triangles). The black dots have historical Th isotope data from cruise 92G07, with station number indicated (Guo et al., 1995). Overlain are schematic representations of surface (black arrows) and deep (blue arrows) circulation patterns from Hamilton et al., (2018) and the climatological extent of the Mississippi-Atchafalya River System (MARS) plume (green dotted line), defined as 50% frequency of salinity less than 31 (da Silva & Castelao, 2018).

The trace metal thorium is supplied to the ocean predominantly from lithogenic sources. In this study we ask the question, can the thorium cycle provide useful information on the balance of sources for lithogenic metals in the Gulf of Mexico? Unfortunately, all continental sources are known to supply dissolved ^{232}Th to seawater (Hayes et al., 2013, 2017; Huh & Bacon, 1985). In the remote ocean, one can usually assume the dominant source is atmospheric dust input because Th has a short residence time (years) with respect to its removal by adsorption onto sinking particles, limiting its lateral transport from other coastal sources (Anderson et al., 2016; Hsieh et al., 2011). Furthermore, atmospheric dust deposition is significant for biological iron requirements since it can be

directly supplied to the euphotic zone. Dissolved ^{232}Th in the Gulf of Mexico, however, is likely to be sourced from a mixture of several continental sources. Our strategy in this study is to compare observed dissolved Th distributions in the northern Gulf of Mexico with that observed in the remote western North Atlantic, which likely receives only a North African dust source. As a preliminary investigation, this comparison can approximate an upper bound on the importance of North African dust as a lithogenic source of ^{232}Th and Fe in the northern Gulf of Mexico. Future studies will be necessary to better quantify metal fluxes associated with North African dust deposition, as well riverine discharge, submarine groundwater discharge, and diffusion from sediments in the Gulf of Mexico, all of which are likely significant. We further estimate the residence time of dissolved Fe in the Gulf of Mexico based on a ^{232}Th-based supply to demonstrate the sensitivity of iron supplies to potential changes in lithogenic supply.

2 Materials and Methods

2.1 Th isotope sampling and analysis in the Gulf of Mexico

Water samples for Th isotopes were collected on two expeditions in the Gulf of Mexico in 2017: cruise PS17-18 (R/V *Point Sur*; April 1, sea surface salinity 36.4) to the site of the former Deepwater Horizon rig (28.72 ˚ N, 88.33 ˚ W) and cruise PE17-24 (R/V *Pelican*; June 26, sea surface salinity 36.5) to the north-central Gulf of Mexico (26.53 ˚ N, 90.83 ˚ W) near the Shell Alcyone Buoy (National Data Buoy Center station 42395). At the time of sampling, these sites were outside the direct influence of the Mississippi-Atchafalaya River Systen (MARS) plume (Fig. 1), using a definition of salinity >31 (da Silva & Castelao, 2018). The MARS plume is also usually characterized by elevated chlorophyll *a* concentrations and satellite images confirm that the sampling sites were outside the plume (Figs. S1 and S2). The interior Gulf of Mexico can be influenced by a northwestward extension of the Loop Current, anticyclonic Loop Current eddies shed from the Loop Current, or cyclonic eddies that can interact with Loop Current eddies and coastal waters. At the time of sampling, site PS17-18 was not influenced by a coherent eddy based on maps of sea-surface height (Supplemental Figs. S3 and S4), and site PE17-24 was near the center of a Loop Current eddy. Thus both sites likely represent the oligotrophic waters of the northern Gulf of Mexico.

Water samples were filtered from a conventional Niskin bottle rosette with 0.45 m Acropak 500 cartridges into 4 L acid-washed cubitainers, following GEO-TRACES protocols (Cutter et al., 2017). Filtered water samples were acidified to 0.024 M HCl with Optima HCl (Fisher) once they were returned to the laboratory and left to sit acidified for at least 2 months before being analyzed to recover any adsorptive loss of Th. Using methods described in Hayes et al. (2017), Th in water samples was pre-concentrated using iron oxyhydroxide coreciptation after addition of yield tracer ^{229}Th, centrifugation, acid digestion (HNO$_3$, HCl, HF and H$_2$O$_2$) of the precipitate, and column chromatography using anion-exchange resin AG1-X8. Th isotope concentrations were determined by isotope

dilution inductively-coupled plasma mass spectrometry on a Thermo-Fisher Element XR. These data are publicly available (Hayes, 2020a, 2020b). Precision on these analyses averaged 1.2% for ^{232}Th and 10.4% for ^{230}Th, with blank corrections representing < 5% of the sample size for ^{232}Th and < 9% for ^{230}Th. Accuracy was assessed using analysis of the GEOTRACES standard solution SWS2010-1 (Anderson et al., 2012). Our results for SWS2010-1 (n = 4) during these analysis were 1005 ± 15 pg/g ^{232}Th and 245 ± 22 fg/g ^{230}Th, within error of the reported intercalibration values. Measured concentrations for ^{230}Th were corrected to the time of sampling, accounting for ingrowth from ^{234}U decay during sample storage.

We present our new data along with published dissolved ^{232}Th and ^{230}Th data from July 1992 (cruise 92G07) in the northwest Gulf of Mexico (Guo et al., 1995), including 1 deep profile at station 5 (92G07-05) and 3 surface stations between there and the Texas coast (Fig. 1). Satelitte information was not available for this 1992 time period to determine the eddy field. The deep site, 92G07-05, and station 4 had a surface salinity of ~36 and station 3 was 32.5, indicating the absence of a river plume influence using the S < 31 threshold. Only station 92G07-01 had surface salinity below 31 (at 30.6). This station is also near the edge of the 50% occurrence line of MARS plume (da Silva & Castelao, 2018; Fig. 1) and thus may have had some riverine influence.

2.2 Deriving dissolved ^{232}Th flux

The residence time of dissolved Th with respect to scavenging removal from an integrated water column (τ_{dTh}) can be derived from the budget of dissolved ^{230}Th assuming sources from ^{234}U decay, advection and diffusion:

$$\tau_{dTh} = \frac{\int d^{230}Th_{xs}\ dz}{P\ +\ AD}\ (1)$$

Here, $\int d^{230}Th_{xs}\ dz$ is the integrated inventory of dissolved ^{230}Th corrected for lithogenic sources (denoted with "xs"). This correction is based on measured dissolved ^{232}Th, assuming a 4 ppm ratio of ^{230}Th/^{232}Th in lithogenic material (Roy-Barman et al., 2002). P is the integrated production rate of ^{230}Th by ^{234}U decay, and AD represents any integrated sources or sinks due to advection or diffusion. In the case of the Gulf of Mexico, we have ignored advective or diffusive sources of ^{230}Th, as there appear to be relatively weak lateral gradients in dissolved ^{230}Th in the deep Gulf (Sec. 3.1). The deep Gulf contains persistent deep gyre circulation (Hamilton et al., 2018) as well as a high degree of isopycnal and diapycnal diffusivity compared to the open ocean (Ledwell et al., 2016), leading to relatively efficient mixing of deep Gulf waters. Once τ_{dTh} is calculated, we can then calculate the integrated input flux of dissolved ^{232}Th (F$_{d232}$; Eq. 2).

$$F_{d232} = \frac{\int d^{232}Th\ dz}{\tau_{dTh}}\ (2),$$

where $\int d^{232}Th\ dz$ is the inventory of dissolved ^{232}Th integrated over the same depth range as in calculating τ_{dTh}. The integration is done from the surface

to a depth of interest, assuming a steady-state balance of Th isotopes within that depth range. The depth of interest is chosen based on the process to be quantified. For instance, studies focusing on atmospheric dust input have chosen depth horizons such as 500 m or 250 m, above which dissolved ^{232}Th input is assumed to be due solely to dissolution of atmospheric dust (Hayes et al., 2013, 2017; Hsieh et al., 2011; Lopez et al., 2015). This is likely a good assumption in the remote ocean; however, benthic and other margin sources of ^{232}Th are documented in some areas (e.g., Pérez-Tribouillier et al., 2020) which would add to the derived flux.

2.3 Distinguishing lithogenic and dust sources in the Gulf of Mexico

In the case of the Gulf of Mexico, the measured flux of dissolved ^{232}Th itself does not indicate its component sources. We can, however, look to remote western North Atlantic sites that are upwind of the North African dust source as an upper bound on the North African dust source that our northern Gulf of Mexico sites might be receiving. Any dissolved ^{232}Th flux measured in the Gulf of Mexico in excess of the remote North Atlantic estimate would therefore be attributable to sources from North America and its margins. For North Atlantic sites, we use Th isotope data from GEOTRACES section GA03, stations KN204-1-10 (coincident with the Bermuda Atlantic Time-series Station, or BATS) and KN204-1-12 (Hayes et al., 2018), both found in the oligotrophic waters of the Sargasso Sea, collected in November 2011. These stations are denoted GA03-10 and GA03-12, for short (see Fig. 2 for map). In this section we provide further jusitication for our assumption of the North Atlantic sites as an upper bound for Saharan dust in our Gulf of Mexico sites from (1) available dust deposition observations and (2) the dust deposition ranges predicted in global models. This assumption is of course only a working assumption for this initial investigation into the lithogenic sources in the Gulf of Mexico. The balance of lithogenic sources if the Gulf deserves further scrutiny as more observations in the region become available.

Our first expectation based simply on proximity to North Africa is that the GA03 stations likely receive a similar or larger amount of North African dust deposition compared to our northern Gulf of Mexico sites. The only available direct observations of bulk dust deposition (wet and dry deposition) in the region are in Miami (Prospero et al., 1987) of 1.26 g/m^2/yr (average over 1982-1983), near Bermuda (Jickells et al., 1998) of 1.9 g/m^2/yr (averaged over 1981-1991, ranging from 1.3 to 3.4 g/m^2/yr interannually) and from a suite of 10 sites throughout the state of Florida (Prospero et al., 2010) that averaged 2.0 g/m^2/yr (1994-1996). Based on these observations alone, it appears that the regions spanning the eastern Gulf of Mexico to Bermuda receive subequal amounts of North African dust deposition, within an uncertainty of about a factor of 2.

For more detail on the expected relative rates of dust deposition between the western North Atlantic and the northern Gulf of Mexico, we make use of an improved representation of global dust deposition (Kok et al., 2021b) that is constrained by surface dust concentration and deposition measurements as well

as satellite-derived dust-aerosol optical depth. This product provides 1 sigma uncertainties for each gridded estimation as well as an estimate of the fractional contribution of the deposition from the world's different dust sources (Kok et al., 2021a). We show the estimates from this product in Figure 2, using the annual total (wet+dry) deposition of PM20 (particulate matter greater than 20 m in geometric diameter), along with the locations of our study sites. Overall, in the region between Bermuda and South Florida, this product agrees well with the available deposition constraints of 1-2 g/m^2/yr. However, the dust product also suggests significant deposition of North American dust (coming from the southwestern US and northeastern Mexico), particularly in the northwestern quandrant of the Gulf of Mexico. We point out that this result is based largely on the observations of satellite optical dust in the area, as the closest deposition measurement constraints for this source are from the southwestern US (Reheis, 2006). There is other evidence that suggests because of the dynamics of the southwestern monsoon, relatively little of the North American dust is deposited in the Gulf of Mexico (Zhao et al., 2012). In August 2014, it was observed that 19-48% of PM2.5 at Houston and Galveston was African dust during a 9-day episode (Bozlaker et al., 2019). The remainder of aerosol sources were mainly anthropogenic aerosols such as road dust and vehicle emissions, with little indication of Southwest US dust. Further regional measurements of aerosols along the Gulf Coast would be helpful for constraining the importance of North American aerosol sources. Nontheless, of our study sites, we suspect that the northwestern Gulf site 92G07-05 would be most likely to receive significant amounts of North American dust deposition, and the other two sites less so.

Looking in more detail at the Kok et al. (2021a,b) dust estimates at our sites illustrates the uncertainty in predicting depositon rates, yet they are still broadly consistent with the assumption of the North Atlantic sites as an upper bound on North African supply to the Gulf. At the model grid nodes nearest the GA03 sites, the range of dust deposition predicted, including 1 sigma uncertainty, is 0.5 to 2.1 g/m^2/yr, of which 50-70% is North African (i.e., 0.3 to 1.3 g/m^2/yr North African dust). For our two north-central Gulf sites, the product gives a range of 0.5 to 6.4 g/m^2/yr dust deposition, of which 30-40% is North African in origin (equal to 0.2 and 2.2 g/m^2/yr North African dust). It is also worth noting that uncertainty in local dust deposition can be even larger in other available global deposition models (Albani et al., 2014). Given the large uncertainties in the model predictions, it is difficult to precisely quantify the relative rates of North African dust deposition at our study sites. Nonetheless, we use the more modest assumption of the North Atlantic sites as an upper bound on North African dust contribution to the northern Gulf sites to perform an initial investigation into the balance of lihtogenic sources implied by the ^{232}Th flux observations.

Finally, with regard to seasonal cycling, neither the GA03 sites (November) or PS17-18 (early April) were sampled in the June-July-August timeframe when Saharan dust makes its most northwestward extension, causing, for example a predicitable increase in surface dust concentrations in Miami (Zuidema et al.,

2019). PE17-24 was sampled in this summer time frame (late June). However, because the residence time of dissolved Th is typically a year or longer in the mixed layer of the open ocean and longer at depth (Hayes et al., 2018; Hayes, Fitzsimmons et al., 2015), we expect seasonal patterns to be largely averaged out in dissolved ^{232}Th concentrations and fluxes. Interannual differences between 2011 and 2017 (6 years) could, however, be expected. There is evidence from the Miami time-series that there was a higher Saharan dust load in the region in 2011 compared to 2017 (Zuidema et al., 2019). This evidence reinforces the concept that the GA03 sampling represents an upper bound on the magnitude of North African dust deposited on the Gulf.
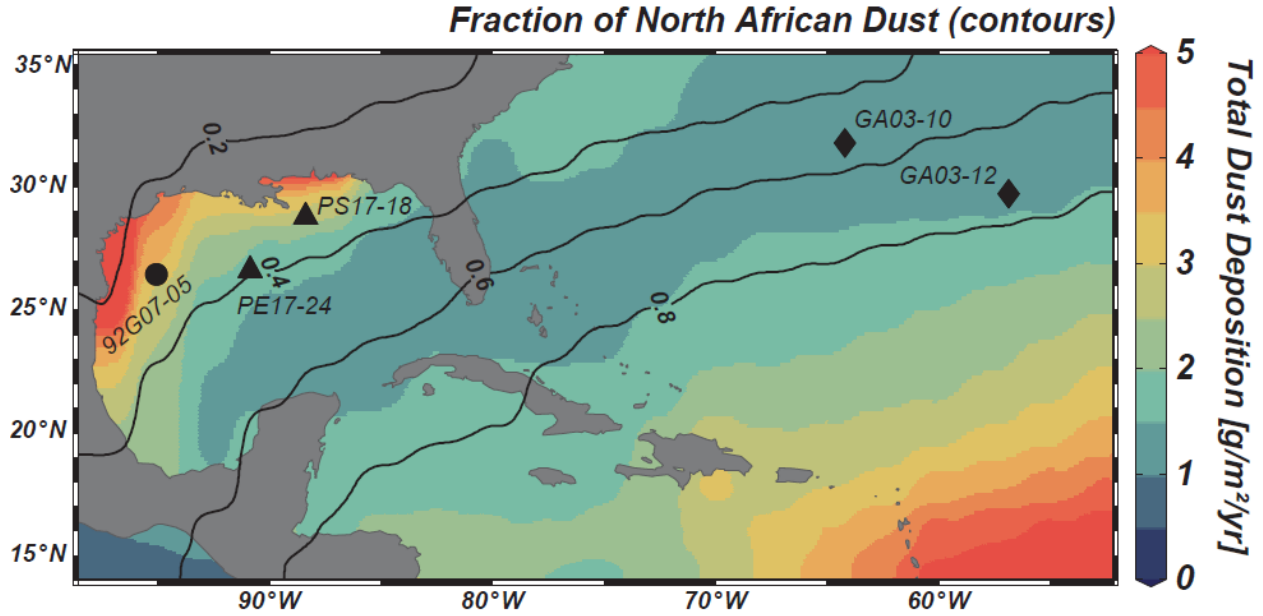

Figure 2. Thorium isotope study sites as plotted in Figure 1 for the Gulf of Mexico (black circle is 92G07-05 from Guo et al., 1995 and black triangles are PS17-18 and PE17-24 from this study) as well as the western North Atlantic sites from GEOTRACES GA03 transect (black diamonds, Hayes et al., 2018). The colormap shows the total (wet plus dry) PM20 deposition from Kok et al. (2021b) and the contours are the fraction of that deposition sourced from North Africa (combining source area numbers 1 thru 3 from Kok et al., 2021a). The balance of depositional fraction is largely made up from North American dust in this dust product.

2.4 Extrapolating to the iron cycle from dissolved ^{232}Th flux

In addition to assessing overall lithogenic sources, the measured flux of dissolved ^{232}Th can be converted into the flux of other specific elements, defined in the present case for dissolved Fe (Eq. 3). This approach assumes an Fe/Th ratio of

the source material (Fe/Th$_\text{source}$) and the relative fractional solubility of the two elements (S$_\text{Fe}$/S$_\text{Th}$). Here we use an Fe/Th ratio of 15,700 $\pm$ 200 mol/mol and S$_\text{Fe}$/S$_\text{Th}$ = 1 $\pm$ 0.4, consistent with observations of North Atlantic aerosol and aerosol leaches, respectively (Hayes et al., 2018; Shelley et al., 2018). There are few available measurements of S$_\text{Fe}$/S$_\text{Th}$ and some recent measurements suggest S$_\text{Fe}$/S$_\text{Th}$ could be as low as 0.2-0.3 (Baker et al., 2020; Roy-Barman et al., 2021). It may be that these operationally defined fractional solubilities are significantly method-dependent. Thus we acknowledge our assumed 40% uncertainty in this parameter may be an underestimate. As Eq. 3 is a linear conversion, our approach assumes that the balance of different dissolved ^{232}Th sources applies to dissolved Fe as well. North American margin sources (including North American dust) could have different Fe/Th composition and solubility ratios; we do not have constraints on this at present and this is a goal for future work. In particular, because Th is not redox sensitive in seawater while Fe is, dissolution of Fe from anoxic/suboxic settings is likely not represented by dissolved Th fluxes. In addition, Fe emissions from combustion aerosols (e.g., Matsui et al., 2018) likely are not co-occuring with Th emissions. In this sense the dissolved Fe fluxes derived from Eq. 3 likely represent oxic dissolution of lithogenic material and only a fraction of the total sources of dissolved Fe.

$$F_\text{dFe} = F_{d232} \times \left(\tfrac{\text{Fe}}{\text{Th}} \right)_\text{source} \times \left(\tfrac{S_\text{Fe}}{S_\text{Th}} \right) \ (3)$$

Finally, to assess the residence time of dissolved iron (τ_dFe), we compare the inventory of dissolved iron $\int$ dFe dz measured in the Gulf of Mexico with our estimated dissolved iron flux (Eq. 4). This also produces an estimate as a function of integrated depth; e.g., a flux integrated to 500 m would be used to estimate τ_dFe in the upper 500 m of the water column, etc. For iron data in the deep northern Gulf of Mexico, we use the deep water survey of the former site of the Deepwater Horizon oil rig (Joung & Shiller, 2013). These authors determined that the 2010 oil spill at this site did not significantly affect Fe distributions there, and at the time of this writing these are the only published observations of dissolved Fe in the Gulf of Mexico deeper than 500 m (see review by Hayes et al., 2019). For dissolved Fe in the GA03 North Atlantic stations, we use the data from Conway & John (2014).

$$\tau_\text{dFe} = \tfrac{\int \text{dFe dz}}{F_\text{dFe}} \ (4)$$

3 Results and Discussion

3.1 Hydrography

The hydrography of the three Gulf of Mexico profiles presented here are relatively similar (Figure 3 and 4a). These subtropical surface waters ranged from 22 $^\circ$C to 29 $^\circ$C in potential temperature and 36.0 to 36.4 in practical salinity. Mixed layers were relatively shallow ($<$ 30 m, defined by 0.125 kg/m^3 increase in potential density from the surface value), giving way to some increases in salinity indicative of Subtropical Underwater within 100-200 m depth and then a permanent thermocline and halocline between 200 m and 800 m depth. Salini-

ties as low as 34.8 around 600 m depth are indicative of Antarctic Intermediate Water which has been advected northward throughout the Atlantic and into the Caribbean Sea-Gulf of Mexico system (Hofman & Worley, 1986). Deep waters (>1000 m) are relatively homogenous in temperature and salinity in the Gulf of Mexico, largely reflecting the character of North Atlantic Deep Water that has entered deep passages in the Caribbean Sea and flowed over the Yucatan sill into the Gulf after some mixing with Caribbean mid-waters (Morrison et al., 1983). The main distinguishing characteristic when comparing the Gulf of Mexico hydrography with that in the western North Atlantic sites shown is the more prominent presence of the 18-degree mode water (Worthington, 1959) between 200 and 600 m depth (Fig. 4a).
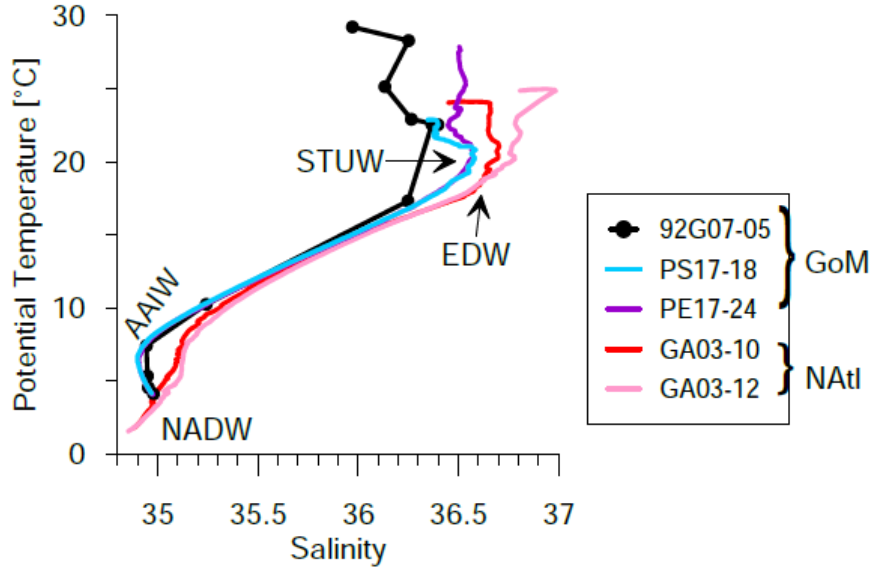

Figure 3. Temperature-Salinity diagram of the 5 deep sites shown in Fig. 2 in the Gulf of Mexico (GoM) and North Atlantic (NAtl). Only discrete bottle values were available for station 92G07-05. All sites show evidence of warm, subtropical surface waters, Subtropical Underwater (STUW) just below the surface, and North Atlantic Deep Water (NADW) at depth. The Sargasso Sea sites (GA03-10 and -12) had more prominent 18°C water (EDW) in the thermoclinate and the Gulf sites had more clear evidence of the salinity minimum associated Antarctic Intermediate Water (AAIW) that has traveled northward through the Caribbean.
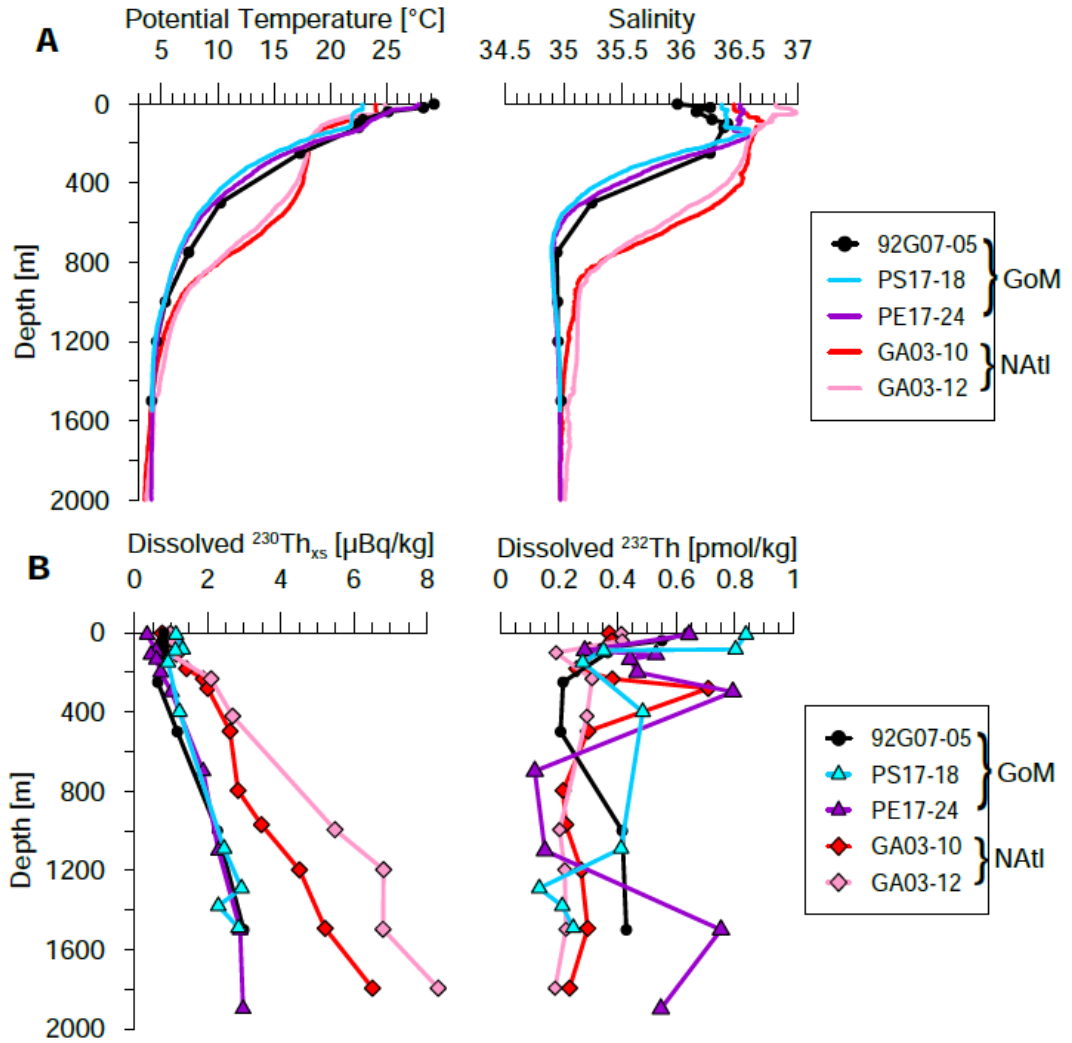
10

Figure 4. (a) Potential temperature and practical salinity and (a) dissolved $^{230}Th_{xs}$ and dissolved ^{232}Th as a function of water depth at the Gulf of Mexico (GoM) and North Atlantic (NAtl) sites indicated in Figure 2. Error bars on the thorium data are smaller than or equal to the symbol size.

3.2 ^{230}Th activity profiles

The depth profiles of $d^{230}Th_{xs}$ presented here (Fig. 4b) all demonstrate a roughly linear increase with depth, consistent with the model of reversible scavenging (Bacon & Anderson, 1982) in which the uniformly produced ^{230}Th undergoes cycles of adsorption and desorption onto settling particles, allowing relatively little lateral transport. There is, however, variability in the upper water column (< 200 m depth), with mixed layer $d^{230}Th_{xs}$ ranging from 0.35

Bq/kg at PE17-24 to 1.14 Bq/kg at PS17-18. This range more than spans the range seen in the mixed layer of the western North Atlantic stations (0.3 to 0.4 Bq/kg) and could potentially be related to surface circulation patterns, such as upwelling, downwelling, vertical mixing, or real differences in particle flux at the sites. The dissolved Th residence times implied by the mixed layer $d^{230}Th_{xs}$ at these sites is 0.8 to 2.6 years (Fig. 5). These timescales suggest that seasonal patterns in particle flux will largely be averaged out. It may also be that vertical mixing or upwelling is supplying a variable magnitude of upward ^{230}Th flux (Luo et al., 1995; Pavia et al., 2020). This effect has important implications for the calculation of dissolved Th fluxes and is discussed more in section 3.4.

Despite variability in the upper 200 m, there are clearly distinct slopes in the $d^{230}Th_{xs}$ profiles between the Gulf of Mexico and the western North Atlantic data. At about 1500 m, there is about 2 times as much $d^{230}Th_{xs}$ at the North Atlantic sites compared to the Gulf sites, indicating reduced scavenging removal by lower particulate fluxes in the remote Atlantic sites. The $d^{230}Th_{xs}$ concentrations at GA03-12 below 500 m are about 20% larger than at GA03-10 and this may be due to a combination of a younger ventilation age at the more northern site (GA03-10) or a slightly lower particle flux at GA03-12 (Hayes, Anderson et al., 2015).

The deep Gulf of Mexico in summer is just as oligotrophic as the Sargasso Sea (Howe et al., 2020; Muller-Karger et al., 1991; Stukel et al., 2021), though the northern Gulf can sometimes be impacted by Mississippi River outlow (Kil et al., 2014; da Silva & Castelao, 2018) potentially leading to a higher annual average biological particle flux in the northern Gulf. Futhermore, the proximity of the extensive continental shelf and slope to the Gulf of Mexico sites (Fig. 1) implies higher total lithogenic particles fluxes, including resuspended nepheloid layers (Diercks et al., 2018), in the Gulf compared to the Sargasso Sea. Thus, both increased biological and lithogenic particulate fluxes likely contribute to greater scavenging removal of $d^{230}Th_{xs}$ at the Gulf sites compared to the remote Atlantic sites. The dissolved Th residence time (Fig. 5) at all three Gulf sites is 1-2 years in surface water and increases linearly with integration depth to about 4 years at 1500 m depth. In comparison at 1500 m depth the Th residence times increase to 8-11 years at the Sargasso Sea sites.

3.3 ^{232}Th concentration profiles

For a tracer supplied predominantly at the surface, say through atmospheric dust, the reversible scavenging model predicts a constant concentration with depth, as the adsorption-desorption balance on particles continues throughout the water column. The profiles of $d^{232}Th$ presented here (Fig. 4b) are not constant with depth, indicating subsurface sources of ^{232}Th such as lateral advection of waters from areas of benthic sediment resuspension, and likely more so for the Gulf of Mexico sites compared with the North Atlantic sites. Beam transmission data would have been useful to support the inference of lateral transport but unfortunately it was not available from the Gulf of Mexico CTD casts. It is worth noting that in contrast to the relative homogeneity of ^{230}Th,

the larger spatial gradients in ^{232}Th seen here do imply that advection and diffusion in the Gulf could physically transport ^{232}Th to regions other than where it was first introduced into seawater.

Significant increases in d^{232}Th concentration near the surface in profiles from PS17-18 and PE17-24 could reflect dust deposition but also could indicate lateral sources as well. Near surface d^{232}Th concentrations are about 30% higher in PS17-18 than in PE17-24, possibly reflecting a coastal shelf source for PS17-18, which is by proximity closer to the northern Gulf Coast. Surface waters of PE17-24 were within a Loop Current eddy (Fig. S4) and thus this water had been relatively recently advected from the Caribbean Sea and may have inheritied the effects of North African dust deposited in the Caribbean (Fig. 2) and/or other Caribbean margin sources such as the Amazon/Orinoco outflows (Hayes et al., 2017). In the northwestern Gulf, Guo et al. (1995) found that surface water d^{232}Th increased from ~0.6 pmol/kg at 92G07 stations 5 and 4 to 1.3 and 1.4 pmol/kg at stations 3 and 1, respectively, station 1 having evidence for MARS influence (see Fig. 1). This is one indication of a riverine/coastal source of d^{232}Th in this sector. Seasonality could possibly play a role in the observed variability within the Gulf of Mexico stations, as the Saharan dust plume reaches is most northwestward extent in summer (Prospero, 1999; Prospero et al., 1987; 2010). However, with dissolved Th residence times around 1 year in the mixed layer and longer at depth (Fig. 5, sec. 3.2), it would be expected that seasonal effects would largely be averaged out. Therefore interannaul (in the case of PS17-18/PE17-24 versus 92G07) or spatial variations are more likely to be responsible for the dissolved ^{232}Th variations seen here.

The average d^{232}Th concentration at all of the Gulf sites (~0.43 pmol/kg) is about 40% higher than the average of the North Atlantic sites (~0.30 pmol/kg in the upper 1800 m of the water column). Furthermore the increased scavenging intensity in the Gulf evidenced by the ^{230}Th data means that there must be a much higher flux of d^{232}Th into the Gulf than the North Atlantic sites to support the dissolved concentrations observed.
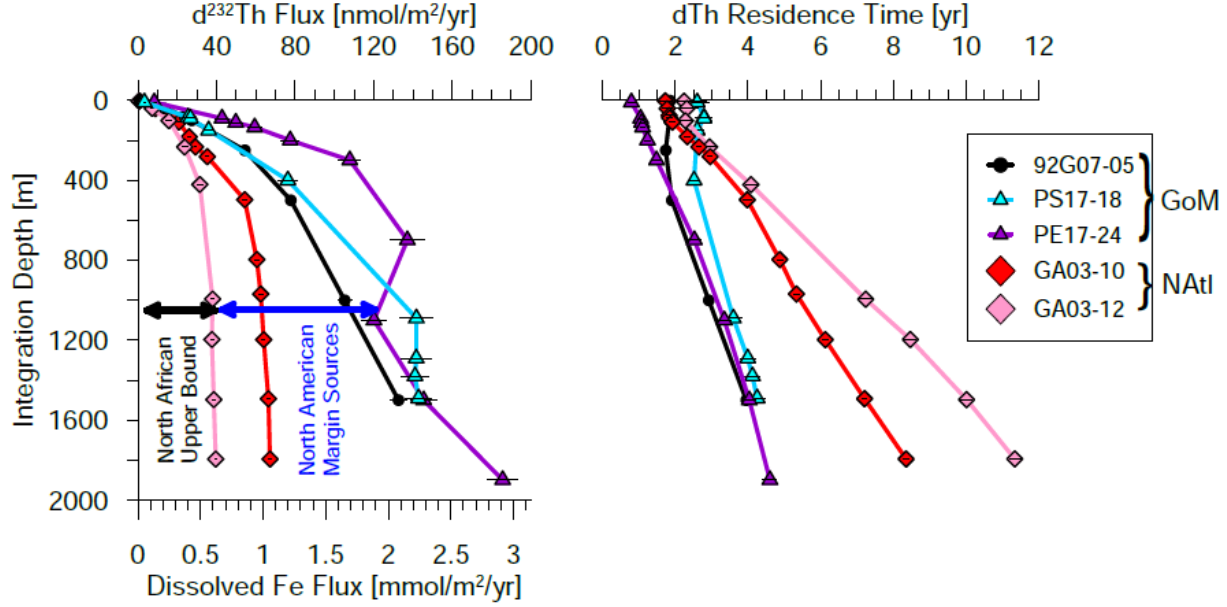
13

Figure 5. (left) Dissolved ^{232}Th flux as a function of integration depth from the surface for the sites in Fig. 2. Assuming the observed flux in the Gulf of Mexico (GoM) sites is a combination of North African dust and North American margin sources, the western North Atlantic (NAtl) sites, which receive only North African dust, can be used an approximate upper limit of the North African dust source in the GoM. Note the upper and lower x-axes are linearly related by Eq. 3. Error bars are shown for dissolved ^{232}Th fluxes which are about 5%, while error bars for dissolved Fe fluxes (not shown) are significantly larger, about 40%, mainly due to uncertainty in the relative Fe/Th solubility. (right) Dissolved Th residence time with respect to scavenging based on integrated d^{230}Th$_{xs}$ inventories compared to production by ^{234}U decay.

3.4 Dissolved ^{232}Th fluxes and the balance of lithogenic sources

When converted to flux, the Gulf of Mexico sites indeed have 2-3 times higher dissolved ^{232}Th flux than the North Atlantic sites (Fig. 5). The apparent increasing ^{232}Th fluxes with integration depth in the upper 500 m has been observed in most other sites around the global ocean and may relate to a flaw in our assumptions in defining the residence time of Th. Prior work suggested that ^{230}Th could be scavenged by a different mechanism than ^{232}Th in the euphotic zone where particle flux is greatest (Hayes et al., 2017). However, as mentioned in Sec. 3.2 it seems a more likely explanation is that vertical mixing or advection in the upper water column causes an upward flux of dissolved ^{230}Th into the mixed layer (Luo et al., 1995; Pavia et al., 2020). This causes the apparent ^{230}Th-based residence time to be too high in the upper water column, driving the flux estimate low. Adding to this effect, the vertical concentration gradient of d^{232}Th is often reversed (lower concentrations at depth), resulting

14

in downward mixing of some of the ^{232}Th deposited at the surface.

The net effect is that our estimates of dissolved ^{232}Th (and extrapolated Fe flux) in Fig. 5 are likely too low, especially in the upper 500 m of the water column. Furthermore, unfortunately we cannot resolve in detail how the profile shape of fluxes might look in this upper water column. As more inventory is integrated with depth, the upper water column effects are accounted for since all of the vertically transported Th is integrated together, and dissolved ^{232}Th flux profiles in the remote ocean tend to be relatively constant with increasing integration depth below about 500-1000 m (Hayes et al., 2018; Pavia et al., 2020; Fig. 5). When this is the case, it is fair to assume that the flux achieved around 500-1000 m integration depth is likely similar to the actual flux being received in surface waters. An exception to this, however, occurs when fluxes continue to increase with integration depth toward the seafloor, as in the case of the Gulf of Mexico profiles (Fig. 5). This situation means there must be dissolved ^{232}Th sources at depth (Hayes et al., 2013), indicating some combination of benthic sources. Additionally, it is difficult to extrapolate what flux might have been received only in surface waters since there is not clear break between surface and benthic sources.

Using the integrations to about 1000 m as a deep water reference since this is where d^{232}Th flux in the GA03 stations finally plateaus with integration, the dissolved ^{232}Th flux from the Gulf of Mexico sites ranges from 100 to 140 nmol/m^2/yr. The flux at the North Atlantic sites ranges from 40 to 60 nmol/m^2/yr. While the relative magnitude of North African dust deposition occurring between the western North Atlantic and the northern Gulf is still uncertain, using the smaller of the two North Atlantic fluxes (40 nmol/m^2/yr) and the larger of the two Gulf fluxes (140 nmol/m^2/yr), we estimate an upper bound of 30% of lithogenic sources in the northern Gulf of Mexico being due to North African dust. The same bound would apply to dissolved Fe under our assumptions in Sec. 2. This result translates to the Gulf receiving a dissolved Fe flux from total oxic, lithogenic sources of 1.7-2.2 mmol/m^2/yr, and a likely upper bound of about 0.6 mmol/m^2/yr specifically from North African dust.

3.5 What can we learn about the possible margin sources of Th and Fe in the Gulf?

Our analysis up to this point has focused on determining what relative proportion of the Th and Fe flux in the Gulf of Mexico is due to North African dust deposition. The flux in excess of the North African dust source must be due to North American marginal sources (including possibly North American aerosols), but can we glean any further information here about what sources those might be? Setting aside North American aerosols for the moment, the three remaining candidates are rivers, submarine groundwater discharge (SGD) and diffusion from sediments. Because Fe and Th are very insoluble and particle-reactive, it has often been thought that any riverine sources would be attenuated close to the coast as the river deltas usually provide a high particle flux environment to trap the metals near the shelf (Boyle et al., 1977). While this largely appears to

15

be the case for Fe in the Mississippi-Atchafalaya system (Ho et al., 2019; Joung & Shiller, 2016), we cannot fully rule out the importance of riverine sources. More detailed transects of trace metals from the Gulf of Mexico river plumes to the interior Gulf will be required to fully asses this.

To estimate the flux of trace elements and isotopes (TEI flux) to the ocean due to submarine groundwater discharge, Charette et al. (2016) developed a method based on inverse-model-derived flux of ^{228}Ra from the shelf (Kwon et al., 2014) and the ratio of the relative enrichment between shelf waters and the adjacent open ocean for ^{228}Ra and the TEI of interest (Eq. 5). This approach assumes the ^{228}Ra and TEI of interest in coastal waters are sourced from SGD. While ^{228}Ra is a specific tracer for SGD, the measured TEI in coastal waters could be from multiple sources. In this sense, estimates from this approach are likely maximum values for SGD input.

$$\textbf{TEI flux} = ^{\textbf{228}}\textbf{Ra flux} \times \left(\frac{\text{TEI}_{\text{shelf}} - \textbf{TEI}_{\text{ocean}}}{^{\textbf{228}}\textbf{Ra}_{\text{shelf}} - ^{\textbf{228}}\textbf{Ra}_{\text{ocean}}} \right) \quad (5)$$

The shelf ^{228}Ra flux estimate for the Gulf of Mexico is 11,800 $\pm$ 3,900 dpm/m^2/yr (Charette et al., 2016). For coastal and interior Gulf of Mexico concentrations of dissolved ^{232}Th we use the 92G07 transect (Fig. 1) of 1.4 pmol/kg (shelf) and 0.6 pmol/kg (ocean) (Guo et al., 1995). For ^{228}Ra, we use observations from a similar transect measured in July 1975 of 23.6 dpm/100kg (shelf) and 6.4 dpm/100kg (ocean) (Reid, 1984). Assuming a 20% uncertainty in each of these concentrations (which admittedly may be an underestimate of the true uncertainty since the measurements are sparse), this results in a dissolved ^{232}Th submarine groundwater discharge of 55 $\pm$ 32 nmol/m^2/yr. This is easily a very significant fraction of the observed total Gulf of Mexico d^{232}Th flux of 100-140 nmol/m^2/yr, especially if up to 60 nmol/m^2/yr of this can be attributed to North African dust. Thus, a majority of the implied North American marginal Th flux could be feasibly explained by submarine groundwater discharge. Of course some of the coastal enhancement of dissolved ^{232}Th flux on the northern Gulf shelf may be due to riverine sources and this would reduce our estimate of SGD flux. Direct observations of ^{228}Ra and ^{232}Th in groundwater or immediately offshore of areas with known groundwater seepage will improve our ability to distinguish between riverine and groundwater sources of ^{232}Th.

Estimates of dissolved Fe on the Louisiana Shelf range from 20-50 nmol/kg (Joung & Shiller, 2016) and in surface waters of the interior Gulf the range is 0.3 to 1.5 nmol/kg (Joung & Shiller, 2013). Using the same Ra-based method, we estimate a maximum dissolved Fe flux from submarine groundwater discharge of 2.3 $\pm$ 1.4 mmol/m^2/yr for the northern Gulf of Mexico. Given our estimate of total dissolved Fe flux of 1.7-2.2 mmol/m^2/yr, with perhaps 0.6 mmol/m^2/yr being due to North African dust, SGD could feasibly make up the remainder of the marginal Fe flux. One large uncertainty in this analysis stems from the difficulty in characterizing an overall "coastal" and "interior" concentration of the tracers which could themselves vary significantly in different regions of

the two domains. Additionally, as was the case for ^{232}Th, some of the coastal Fe enrichment may be due to riverine inputs. Better characterizing spatial concentration gradients of radium, thorium and iron in the Gulf of Mexico and relevant groundwater and riverine sources will reduce this uncertainty.

Diffusion from benthic sediments is likely also a significant source in the Gulf of Mexico, though the magnitude is currently highly uncertain. There is evidence for benthic Fe fluxes from both oxic and suboxic/anoxic sediments (Conway & John, 2014; Homoky et al., 2016, 2021). Joung & Shiller (2016) found that the hypoxic Louisiana Shelf could be an Fe source seasonally, though this source could be related to SGD as well. A recent empirically-informed diagenetic model estimated that Gulf of Mexico sediments range from being a sink of dissolved Fe to being a source as high as about 0.5 mmol/m^2/yr (Dale et al., 2015). Benthic chamber experiments in diverse sedimentary environments will narrow this range in the future. In sum, the Gulf of Mexico potentially has significant lithogenic Fe sources from four pathways (aerosols, SGD, rivers and sediments). We note that our measured dissolved ^{232}Th flux likely includes oxic dissolution, but since ^{232}Th is not redox sensitive, this likely neglects any suboxic sedimentary Fe release. Furthermore, ^{232}Th likely has no sources from biomass or fossil fuel burning as iron does (Hamilton et al., 2020).

3.6 Dissolved Fe residence time in the Gulf of Mexico

With the estimated dissolved Fe fluxes and observations of dissolved Fe in these waters, we can calculate the dissolved Fe residence time (or replacement time) with respect to the input. Dissolved Fe was measured directly at sites GA03-10 and -12 (Conway & John, 2014) in November 2011 and at the Deepwater Horizon site (Joung & Shiller, 2013) in May 2010, October 2010 and October 2011 (Fig. 6). The Deepwater Horizon site Fe data was not measured as a vertical profile, but rather deepwater was surveyed at several locations around the rig site. Additionally Joung & Shiller (2013) found that Fe concentrations tended to increase near the seafloor which occurred at a different depth at each particular site. For the residence time calculation, we use a depth-binned average dissolved Fe concentration profile to compare with the flux profile (the depth bins were 1-5 m at the surface, and roughly every 100 m between 600 and 1500 m depth). Within uncertainties, the residence time of dissolved Fe at the Deepwater Horizon site is nearly indistinguishable between that in the western North Atlantic (Fig. 6), ranging from 0.2 ± 0.1 years (or 70 ± 35 days) in the surface to 6 months at depth. The similarity of this residence time to that in the North Atlantic is despite a much larger source term in the Gulf of Mexico (Fig. 5). In other words, the higher input rate of dissolved Fe into the Gulf of Mexico must be balanced by increased removal processes, likely scavenging on to the greater particle flux in the Gulf. This idea could be tested by assessing the adsorbed component of Fe in particulate material (water column or sediment) and we would predict a greater adsorbed component in in the Gulf versus the North Atlantic.
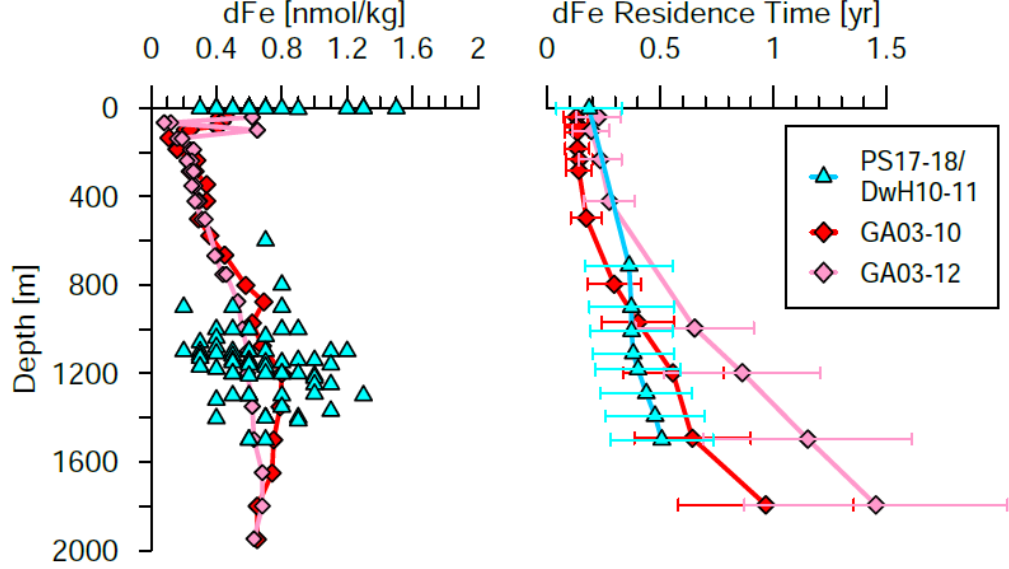
Figure 6. Dissolved iron concentration profiles (left) from the western North Atlantic sites (Conway & John, 2014) and the site of the former Deepwater Horizon in 2010 and 2011 (DwH10-11; Joung & Shiller, 2013) which is roughly coincident with the location of PS17-18 from this study. The DwH study surveyed several sites around the former oil rig, focusing on water depths where the deep oil spill occurred. Dissolved iron residence times (right) were computed using dissolved Fe inventories from the data on the left and the dissolved iron fluxes shown in Fig. 5, with progated uncertainties shown in the colored error bars.

Constraining the residence time of iron in the upper ocean has been a major focus in oceanography since it was realized that iron availability limits the overall productivity in many ecosystems (Landing & Bruland, 1987; Martin & Gordon, 1988) A recent compilation of dissolved Fe residence time estimates suggests that $_{dFe}$ in the upper 250 m of the water column is on the order of sub-annual, consistent with our findings, but there are large variations between studies (Black et al., 2020). A caveat here (as mentioned in Sec. 3.4) is that due to the mixed layer effect on ^{230}Th distributions, our calculated fluxes are likely too low in the upper 500 m. Higher fluxes would reduce the apparent Fe residence time. Furthermore, by defining the residence time with respect to a ^{232}Th-based source, we are also overestimating the residence time since we are neglecting dissolved Fe sources from suboxic sediments and combustion-related aerosols. Thus, particularly in suface waters, we estimate that the dissolved Fe residence time in the Gulf of Mexico is likely considerably less than 2 months. Given that a non-negligible fraction of this iron is sourced from atmospheric dust, seasonal or shorter term dust events are likely to impact Fe availability and could easily

impact phytoplankton community structure, as has been hypothesized on the West Florida Shelf (Lenes et al., 2001; Walsh et al., 2006; Walsh & Steidinger, 2001). That said, temporal changes in submarine groundwater discharge, river discharge or sedimentary diffusion would be equally valid candidates for changing iron supplies, given their likely substantial contributions to the iron budget in the Gulf. Future work determining the impact of iron availability in the Gulf will need to independently assess at least these three major iron sources. The possibility for Fe input from North American lithogenic and anthropogenic aerosols should also be investigated further.

4 Conclusions

In this study, we have mapped the distribution of dissolved ^{232}Th, ^{230}Th and dissolved ^{232}Th flux at three deep sites in the northern Gulf of Mexico. This distribution demonstrates a higher particle scavenging intensity in the Gulf, compared to sites in the adjacent Sargasso Sea, as well as clearly elevated margin sources of ^{232}Th in the Gulf. This total flux likely includes contributions from atmospheric dust, submarine groundwater discharge, riverine discharge and benthic sedimentary release. Using upwind sites in the Sargasso Sea, we suggest an upper bound of 30% for the North African dust contribution to Gulf of Mexico ^{232}Th and Fe supplies. Our thorium-based method neglects some sources of iron including suboxic sediment release and combustion aerosol sources and uncertainties remain in distinguishing the relative role of the remaining North American margin sources. Implied maximum residence times of dissolved iron of about 2 months in the upper 250 m and 6 months in the entire Gulf, clearly indicate the ability of iron supply changes to result in dynamic ecosystem responses. Future work to more accurately determine the spatial concentration gradients of radium and other trace metals of interest between coastal and interior Gulf water and in relevant groundwater and riverine end-members will significantly improve estimates of submarine groundwater discharge sources as well as better constraining the overall budget of lithogenic sources.

Acknowledgments

References

Albani, S., Mahowald, N. M., Perry, A. T., Scanza, R. A., Zender, C. S., Heavens, N. G. et al. (2014). Improved dust representation in the Community Atmosphere Model. *Journal of Advances in Modeling Earth Systems*, *6*, 541–570. https://doi.org/10.1002/2013MS000279Anderson, R. F., Fleisher, M. Q., Robinson, L. F., Edwards, R. L., Hoff, J. A., Moran, S. B. et al. (2012). GEOTRACES intercalibration of ^{230}Th, ^{232}Th, ^{231}Pa, and

prospects for [10]Be. *Limnology and Oceanography: Methods*, *10*, 179–213. https://doi.org/10.4319/lom.2012.10.179Anderson, R. F., Cheng, H., Edwards, R. L., Fleisher, M. Q., Hayes, C. T., Huang, K.-F. et al. (2016). How well can we quantify dust deposition to the ocean? *Philosophical Transactions of the Royal Society A: Mathematical, Physical and Engineering Sciences*, *374*(2081). https://doi.org/10.1098/rsta.2015.0285Bacon, M. P., & Anderson, R. F. (1982). Distribution of thorium isotopes between dissolved and particulate forms in the deep sea. *Journal of Geophysical Research*, *87*(C3), 2045–2056. https://doi.org/10.1029/JC087iC03p02045Baker, A. R., Li, M., & Chance, R. (2020). Trace Metal Fractional Solubility in Size-Segregated Aerosols From the Tropical Eastern Atlantic Ocean. *Global Biogeochemical Cycles*, *34*(6), 1–9. https://doi.org/10.1029/2019GB006510Black, E. E., Kienast, S. S., Lemaitre, N., Lam, P. J., Anderson, R. F., Planquette, H. et al. (2020). Ironing out Fe residence time in the dynamic upper ocean. *Global Biogeochemical Cycles*, 0–3. https://doi.org/10.1029/2020GB006592Boyle, E. A., Edmond, J. M., & Sholkovitz, E. R. (1977). The mechanism of iron removal in estuaries. *Geochimica et Cosmochimica Acta*, *41*, 1313–1324. https://doi.org/10.1016/0016-7037(77)90075-8Boyle, E. A., Reid, D. F., Huested, S. S., & Hering, J. (1984). Trace metals and radium in the Gulf of Mexico: an evaluation of river and continental shelf sources. *Earth and Planetary Science Letters*, *69*, 69–87. https://doi.org/10.1016/0012-821X(84)90075-XBozlaker, A., Prospero, J. M., Price, J., & Chellam, S. (2019). Identifying and Quantifying the Impacts of Advected North African Dust on the Concentration and Composition of Airborne Fine Particulate Matter in Houston and Galveston, Texas. *Journal of Geophysical Research: Atmospheres*, *124*(22), 12282–12300. https://doi.org/10.1029/2019JD030792Charette, M. A., Lam, P. J., Lohan, M. C., Kwon, E. Y., Hatje, V., Jeandel, C. et al. (2016). Coastal ocean and shelf-sea biogeochemical cycling of trace elements and isotopes: lessons learned from GEOTRACES. *Philosophical Transactions of the Royal Society A*, *374*, 20160076.Conway, T. M., & John, S. G. (2014). Quantification of dissolved iron sources to the North Atlantic Ocean. *Nature*. https://doi.org/10.1038/nature13482Cutter, G., Casciotti, K. L., Croot, P., Geibert, W., Heimburger, L.-E., Lohan, M. et al. (2017). Sampling and Sample-handling Protocols for GEOTRACES cruises. Retrieved July 28, 2020, from https://geotracesold.sedoo.fr/images/Cookbook.pdfDale, A. W., Nickelsen, L., Scholz, F., Hensen, C., Oschlies, A., & Wallman, K. (2015). A revised global estimate of dissolved iron fluxes from marine sediments. *Global Biogeochemical Cycles*, *29*, 691–707. https://doi.org/10.1002/2014GB005017Diercks, A. R., Dike, C., Asper, V. L., DiMarco, S. F., Chanton, J. P., & Passow, U. (2018). Scales of seafloor sediment resuspension in the northern Gulf of Mexico. *Elementa: Science of the Anthropocene*, *6*, 1–28. https://doi.org/10.1525/elementa.285Gonneea, M. E., Charette, M. A., Liu, Q., Herrera-Silveira, J. A., & Morales-Ojeda, S. M. (2014). Trace element geochemistry of groundwater in a karst subterranean estuary (Yucatan Peninsula, Mexico). *Geochimica et Cosmochimica Acta*, *132*, 31–49. https://doi.org/10.1016/j.gca.2014.01.037Guo, L., Santschi, P. H., Baskaran,

M., & Zindler, A. (1995). Distribution of dissolved and particulate ^{230}Th and ^{232}Th in seawater from the Gulf of Mexico and off Cape Hatteras as measured by SIMS. *Earth and Planetary Science Letters*, *133*, 117–128.Hamilton, D. S., Scanza, R. A., & Rathod, S. D. (2020). Recent (1980 to 2015) Trends and Variability in Daily-to-Interannual Soluble Iron Deposition from Dust, Fire, and Anthropogenic Sources. *Geophysical Research Letters*, *47*, e2020GL089688. https://doi.org/10.1029/2020GL089688Hamilton, P., Leben, R., Bower, A., Furey, H., & Pérez-Brunius, P. (2018). Hydrography of the Gulf of Mexico using autonomous floats. *Journal of Physical Oceanography*, *48*(4), 773–794. https://doi.org/10.1175/JPO-D-17-0205.1Hayes, C. T. (2020a). Dissolved thorium-230 and thorium-232 from R/V Pelican cruise PE17-24 in the deep Northern Gulf of Mexico during June 2017. *BCO-DMO*, *2020-07–31*. https://doi.org/10.26008/1912/bco-dmo.819622.1Hayes, C. T. (2020b). Dissolved thorium-230 and thorium-232 from R/V Point Sur cruise PS1718 at the site of the former Deepwater Horizon in April 2017. *BCO-DMO*, *2020-07–28*. https://doi.org/10.26008/1912/bco-dmo.819674.1Hayes, C. T., Anderson, R. F., Fleisher, M. Q., Serno, S., Winckler, G., & Gersonde, R. (2013). Quantifying lithogenic inputs to the North Pacific Ocean using the long-lived thorium isotopes. *Earth and Planetary Science Letters*, *383*. https://doi.org/10.1016/j.epsl.2013.09.025Hayes, C. T., Anderson, R. F., Fleisher, M. Q., Huang, K. F., Robinson, L. F., Lu, Y. et al. (2015). ^{230}Th and ^{231}Pa on GEOTRACES GA03, the U.S. GEOTRACES North Atlantic transect, and implications for modern and paleoceanographic chemical fluxes. *Deep Sea Research II*, *116*, 29–41. https://doi.org/10.1016/j.dsr2.2014.07.007Hayes, C. T., Fitzsimmons, J. N., Boyle, E. A., McGee, D., Anderson, R. F., Weisend, R., & Morton, P. L. (2015). Thorium isotopes tracing the iron cycle at the Hawaii Ocean Time-series Station ALOHA. *Geochimica et Cosmochimica Acta*, *169*, 1–16. https://doi.org/10.1016/j.gca.2015.07.019Hayes, C. T., Rosen, J., McGee, D., & Boyle, E. A. (2017). Thorium distributions in high- and low-dust regions and the significance for iron supply. *Global Biogeochemical Cycles*, *31*(2), 328–347. https://doi.org/10.1002/2016GB005511Hayes, C. T., Anderson, R., Cheng, H., Conway, T. M., Edwards, R. L., Fleisher, M. Q. et al. (2018). Replacement Times of a Spectrum of Elements in the North Atlantic Based on Thorium Supply. *Global Biogeochemical Cycles*, *32*(9). https://doi.org/10.1029/2017GB005839Hayes, C. T., Wen, L.-S., Lee, C.-P., Santschi, P. H., & Johannesson, K. H. (2019). Trace Metals in the Gulf of Mexico: Synthesis and Future Directions. In T. S. Bianchi (Ed.), *Gulf of Mexico Origin, Waters and Biota: Volume 5 Chemical Oceanography* (pp. 93–119). College Station, TX: Texas A&M University Press.Ho, P., Shim, M. J., Howden, S. D., & Shiller, A. M. (2019). Temporal and spatial distributions of nutrients and trace elements (Ba, Cs, Cr, Fe, Mn, Mo, U, V and Re) in Mississippi coastal waters: Influence of hypoxia, submarine groundwater discharge, and episodic events. *Continental Shelf Research*, *175*(December 2018), 53–69. https://doi.org/10.1016/j.csr.2019.01.013Hofman, E. E., & Worley, S. J. (1986). An Investigation of the Circulation of the Gulf of Mexico. *Journal of Geophysical Research*, *91*(C12), 14221–14236.

https://doi.org/10.1029/JC091iC12p14221Homoky, W. B., Weber, T., Berelson, W. M., Conway, T. M., Henderson, G. M., Van Hulten, M. et al. (2016). Quantifying trace element and isotope fluxes at the ocean-sediment boundary: A review. *Philosophical Transactions of the Royal Society A*, *374*, 20160246. https://doi.org/10.1098/rsta.2016.0246Homoky, W. B., Conway, T. M., John, S. G., König, D., Deng, F. F., Tagliabue, A., & Mills, R. A. (2021). Iron colloids dominate sedimentary supply to the ocean interior. *Proceedings of the National Academy of Sciences of the United States of America*, *118*(13). https://doi.org/10.1073/PNAS.2016078118Howe, S., Miranda, C., Hayes, C., Letscher, R., & Knapp, A. N. (2020). The dual isotopic composition of nitrate in the Gulf of Mexico and Florida Straits. *Journal of Geophysical Research: Oceans*, (3), 1–17. https://doi.org/10.1029/2020jc016047Hsieh, Y.-T., Henderson, G. M., & Thomas, A. L. (2011). Combining seawater ^{232}Th and ^{230}Th concentrations to determine dust fluxes to the surface ocean. *Earth and Planetary Science Letters*, *312*(3–4), 280–290. https://doi.org/10.1016/j.epsl.2011.10.022Huh, C.-A., & Bacon, M. P. (1985). Thorium-232 in the eastern Caribbean Sea. *Nature*, *316*(6030), 718–721. https://doi.org/10.1038/316718a0Jeandel, C. (2016). Overview of the mechanisms that could explain the "Boundary Exchange" at the land-ocean contact. *Philosophical Transactions of the Royal Society A*, *374*, 20150287. https://doi.org/10.1098/rsta.2015.0287Jickells, T. D., Dorling, S., Deuser, W. G., Church, T. M., Arimoto, R., & Prospero, J. M. (1998). Air-borne dust fluxes to a deep water sediment trap in the Sargasso Sea. *Global Biogeochemical Cycles*, *12*, 311–320. https://doi.org/10.1029/97GB03368Joung, D., & Shiller, A. M. (2013). Trace element distributions in the water column near the Deepwater Horizon well blowout. *Environmental Science and Technology*, *47*(5), 2161–2168. https://doi.org/10.1021/es303167pJoung, D., & Shiller, A. M. (2016). Temporal and spatial variations of dissolved and colloidal trace elements in Louisiana Shelf waters. *Marine Chemistry*, *181*, 25–43. https://doi.org/10.1016/j.marchem.2016.03.003Kil, B., Wiggert, J. D., & Howden, S. D. (2014). Evidence That an Optical Tail in the Gulf of Mexico After Tropical Cyclone Isaac was the Result of Offshore Advection of Coastal Water. *Marine Technology Society Journal*, *48*(4), 27–35. https://doi.org/10.4031/mtsj.48.4.4Kinsey, J. C., & German, C. R. (2013). Sustained volcanically-hosted venting at ultraslow ridges: Piccard Hydrothermal Field, Mid-Cayman Rise. *Earth and Planetary Science Letters*, *380*, 162–168. https://doi.org/10.1016/j.epsl.2013.08.001Kok, J. F., Adebiyi, A. A., Albani, S., Balkanski, Y., Checa-Garcia, R., Chin, M., Colarco, P. R., Hamilton, D. S., Huang, Y., Ito, A., Klose, M., Li, L. et al. (2021). Contribution of the world's main dust source regions to the global cycle of desert dust. *Atmospheric Chemistry and Physics*, *21*(10), 8169–8193. https://doi.org/10.5194/acp-21-8169-2021Kok, J. F., Adebiyi, A. A., Albani, S., Balkanski, Y., Checa-Garcia, R., Chin, M., Colarco, P. R., Hamilton, D. S., Huang, Y., Ito, A., Klose, M., Leung, D. M. et al. (2021). Improved representation of the global dust cycle using observational constraints on dust properties and abundance. *Atmospheric Chemistry and Physics*, *21*(10),

8127–8167. https://doi.org/10.5194/acp-21-8127-2021Kwon, E. Y., Kim, G., Primeau, F., Moore, W. S., Cho, H.-M., Devries, T. et al. (2014). Global estimate of submarine groundwater discharge based on an observationally constrained radium isotope model. *Geophysical Research Letters*, *41*, 8438–8444. https://doi.org/10.1002/2014GL061574Landing, W. M., & Bruland, K. W. (1987). Tbe contrasting biogeochemistry of iron and manganese in the Pacific Ocean. *Geochimica et Cosmochimca Acta*, *51*, 29–43.Ledwell, J. R., He, R., Xue, Z., DiMarco, S. F., Spencer, L. J., & Chapman, P. (2016). Dispersion of a tracer in the deep Gulf of Mexico. *Journal of Geophysical Research: Oceans*, *121*, 110–1132. https://doi.org/10.1002/2015JC011405Lenes, J. M., Darrow, B. P., Cattrall, C., Heil, C. A., Callahan, M., Vargo, G. A. et al. (2001). Iron fertilization and the Trichodesmium response on the West Florida shelf. *Limnology and Oceanography*, *46*(6), 1261–1277. https://doi.org/10.4319/lo.2001.46.6.1261Lopez, G. I., Marcantonio, F., Lyle, M., & Lynch-stieglitz, J. (2015). Dissolved and particulate ^{230}Th–^{232}Th in the Central Equatorial Pacific Ocean: Evidence for far-field transport of the East Pacific Rise hydrothermal plume. *Earth and Planetary Science Letters*, *431*, 87–95. https://doi.org/10.1016/j.epsl.2015.09.019Luo, S., Ku, T. L., Kusakabe, M., Bishop, J. K., & Yang, Y. L. (1995). Tracing particle cycling in the upper ocean with ^{230}Th and ^{228}Th: An investigation in the equatorial Pacific along 140°W. *Deep Sea Research II*, *42*(2–3), 805–829. https://doi.org/10.1016/0967-0645(95)00019-MMartin, J. H., & Gordon, R. M. (1988). Northeast Pacific iron distributions in relation to phytoplankton productivity. *Deep Sea Research*, *35*(2), 177–196.Matsui, H., Mahowald, N. M., Moteki, N., Hamilton, D. S., Ohata, S., Yoshida, A. et al. (2018). Anthropogenic combustion iron as a complex climate forcer. *Nature Communications*, *9*(1). https://doi.org/10.1038/s41467-018-03997-0McCoy, C. A., & Corbett, D. R. (2009). Review of submarine groundwater discharge (SGD) in coastal zones of the Southeast and Gulf Coast regions of the United States with management implications. *Journal of Environmental Management*, *90*(1), 644–651. https://doi.org/10.1016/j.jenvman.2008.03.002McDermott, J. M., Sylva, S. P., Ono, S., German, C. R., & Seewald, J. S. (2018). Geochemistry of fluids from Earth's deepest ridge-crest hot-springs: Piccard hydrothermal field, Mid-Cayman Rise. *Geochimica et Cosmochimica Acta*, *228*, 95–118. https://doi.org/10.1016/j.gca.2018.01.021Mellett, T., & Buck, K. N. (2020). Spatial and temporal variability of trace metals (Fe, Cu, Mn, Zn, Co, Ni, Cd, Pb), iron and copper speciation, and electroactive Fe-binding humic substances in surface waters of the eastern Gulf of Mexico. *Marine Chemistry*, *227*(January), 103891. https://doi.org/10.1016/j.marchem.2020.103891Milliman, J., & Meade, R. (1983). World-wide delivery of river sediment to the oceans. *The Journal of Geology*, *91*(1), 1–21. https://doi.org/10.1086/628741Morrison, J. M., Merrell, W. J., Key, R. M., & Key, T. C. (1983). Property Distribution and Deep Chemical Measurements Within the Western Gulf of Mexico. *Journal of Geophysical Research*, *88*(c4), 2601–2608. https://doi.org/10.1029/JC088iC04p02601Muller-Karger, F. E., Walsh, J. J., Evans, R. H., & Meyers, M. B. (1991). On

the seasonal phytoplankton concentration and sea surface temperature cycles of the Gulf of Mexico as determined by satellites. *Journal of Geophysical Research*, *96*(C7). https://doi.org/10.1029/91jc00787Pavia, F. J., Anderson, R. F., Winckler, G., & Fleisher, M. Q. (2020). Atmospheric Dust Inputs, Iron Cycling, and Biogeochemical Connections in the South Pacific Ocean from Thorium Isotopes. *Global Biogeochemical Cycles*, *34*, e2020GB006562. https://doi.org/10.1029/2020gb006562Pérez-Tribouillier, H., Noble, T. L., Townsend, A. T., Bowie, A. R., & Chase, Z. (2020). Quantifying Lithogenic Inputs to the Southern Ocean Using Long-Lived Thorium Isotopes. *Frontiers in Marine Science*, *7*(April), 1–16. https://doi.org/10.3389/fmars.2020.00207Prospero, J. M. (1999). Long-term measurements of the transport of African mineral dust to the southeastern United States: Implications for regional air quality are also observed. *Journal of Geophysical Research*, *104*, 15917–15927. https://doi.org/10.1029/1999JD900072Prospero, J. M., Nees, R. T., & Uematsu, M. (1987). Deposition rate of particulate an dissolved aluminum derived from Saharan dust in precipitation in Miami, Florida. *Journal of Geophysical Research*, *92*, 14723–14731. https://doi.org/10.1029/JD092iD12p14723Prospero, J. M., Landing, W. M., & Schulz, M. (2010). African dust deposition to Florida: Temporal and spatial variability and comparisons to models. *Journal of Geophysical Research*, *115*, D13304. https://doi.org/10.1029/2009JD012773Reheis, M. C. (2006). A 16-year record of eolian dust in Southern Nevada and California, USA: Controls on dust generation and accumulation. *Journal of Arid Environments*, *67*(3), 487–520. https://doi.org/10.1016/j.jaridenv.2006.03.006Reid, D. F. (1984). Radium variability produce by shelf-water transport and mixing in the western Gulf of Mexico. *Deep Sea Research*, *31*(12), 1501–1510. https://doi.org/10.1016/0198-0149(84)90084-0Roy-Barman, M., Coppola, L., & Souhaut, M. (2002). Thorium isotopes in the western Mediterranean Sea: An insight into the marine particle dynamics. *Earth and Planetary Science Letters*, *196*(3–4), 161–174. https://doi.org/10.1016/S0012-821X(01)00606-9Roy-Barman, M., Foliot, L., Douville, E., Leblond, N., Gazeau, F., Bressac, M. et al. (2021). Contrasted release of insoluble elements (Fe, Al, rare earth elements, Th, Pa) after dust deposition in seawater: A tank experiment approach. *Biogeosciences*, *18*(8), 2663–2678. https://doi.org/10.5194/bg-18-2663-2021Shelley, R. U., Landing, W. M., Ussher, S. J., Planquett, H., & Sarthou, G. (2018). Characterisation of aerosol provenance from the fractional solubility of Fe (Al, Ti, Mn, Co, Ni, Cu, Zn, Cd and Pb) in North Atlantic aerosols (GEOTRACES GA01 and GA03). *Biogeosciences*, 1–31. https://doi.org/10.5194/bg-2017-415da Silva, C. E., & Castelao, R. M. (2018). Mississippi River Plume Variability in the Gulf of Mexico From SMAP and MODIS-Aqua Observations. *Journal of Geophysical Research: Oceans*, *123*(9), 6620–6638. https://doi.org/10.1029/2018JC014159Stukel, M. R., Kelly, T. B., Landry, M. R., Selph, K. E., & Swalethorp, R. (2021). Sinking carbon, nitrogen, and pigment flux within and beneath the euphotic zone in the oligotrophic, open-ocean Gulf of Mexico. *Journal of*

Plankton Research, 1–17. https://doi.org/10.1093/plankt/fbab001Tagliabue, A., Bowie, A. R., Philip, W., Buck, K. N., Johnson, K. S., & Saito, M. A. (2017). The integral role of iron in ocean biogeochemistry. *Nature*, *543*(7643), 51–59. https://doi.org/10.1038/nature21058Tang, D., Warnken, K. W., & Santschi, P. H. (2002). Distribution and partitioning of trace metals (Cd, Cu, Ni, Pb, Zn) in Galveston Bay waters. *Marine Chemistry*, *78*(1), 29–45. https://doi.org/10.1016/S0304-4203(02)00007-5Walsh, J. J., & Steidinger, K. A. (2001). Saharan dust and Florida red tides: The cyanophyte connection. *Journal of Geophysical Research*, *106*(C6), 11597. https://doi.org/10.1029/1999JC000123Walsh, J. J., Jolliff, J. K., Darrow, B. P., Lenes, J. M., Milroy, S. P., Remsen, A. et al. (2006). Red tides in the Gulf of Mexico: Where, when, and why? *Journal of Geophysical Research: Oceans*, *111*(11), 1–46. https://doi.org/10.1029/2004JC002813Wen, L.-S., Santschi, P. H., Warnken, K. W., Davison, W., Zhang, H., Li, H. P., & Jiann, K. T. (2011). Molecular weight and chemical reactivity of dissolved trace metals (Cd, Cu, Ni) in surface waters from the Mississippi River to Gulf of Mexico. *Estuarine, Coastal and Shelf Science*, *92*(4), 649–658. https://doi.org/10.1016/j.ecss.2011.03.009Worthington, L. V. (1959). The 18° water in the Sargasso Sea. *Deep Sea Research*, *5*, 297–305. https://doi.org/10.1016/0146-6313(58)90026-1Yingling, N., Kelly, T. B., Shropshire, T. A., Landry, M. R., Selph, K. E., Knapp, A. N. et al. (2021). Taxon-specific phytoplankton growth, nutrient utilization and light limitation in the oligotrophic Gulf of Mexico. *Journal of Plankton Research*, 1–21. https://doi.org/10.1093/plankt/fbab028Zhao, C., Liu, X., & Leung, L. R. (2012). Impact of the Desert dust on the summer monsoon system over Southwestern North America. *Atmospheric Chemistry and Physics*, *12*(8), 3717–3731. https://doi.org/10.5194/acp-12-3717-2012Zhao, Y., & Quigg, A. (2014). Nutrient limitation in Northern Gulf of Mexico (NGOM): Phytoplankton communities and photosynthesis respond to nutrient pulse. *PLoS ONE*, *9*(2). https://doi.org/10.1371/journal.pone.0088732Zuidema, P., Alvarez, C., Kramer, S. J., Custals, L., Izaguirre, M., Sealy, P. et al. (2019). Is summer African dust arriving earlier to Barbados? *Bulletin of the American Meteorological Society*, *100*(10), 1981–1986. https://doi.org/10.1175/BAMS-D-18-0083.1